

# Real-space computation of $E/B$ -mode maps I: Formalism and Compact Kernels

**Aditya Rotti and Kevin Huffenberger**

Department of Physics, Florida State University, Keen Physics Building, 77 Chieftan Way, Tallahassee, Florida, U.S.A.

E-mail: [adityarotti@gmail.com](mailto:adityarotti@gmail.com), [khuffenberger@fsu.edu](mailto:khuffenberger@fsu.edu)

**Abstract.** We derive full-sky, real-space operators that convert between polarization Stokes  $Q/U$  parameters to the coordinate-independent, scalar  $E/B$  modes that are widely used in Cosmic Microwave Background and cosmic shear analysis. The convolution kernels split naturally into angular and radial parts, and we show explicitly how the spatial extent of the convolution kernel depends on the targeted band-limit. We show that an arbitrary radial dependence can produce  $E/B$ -like maps and that these are simply filtered versions of the standard  $E/B$  maps. This allows us to compute  $E/B$  maps in real space with a compactly-supported kernel, an approach that can guarantee the avoidance of known foreground regions and can be employed in a massively parallel scheme at high-resolution. We can compute power spectra using standard techniques, and recover the power spectrum of the sky with a simple window function. We cast the standard CMB polarization analysis operators in a matrix-vector notation which facilitates the derivations and shows that the kernels relate directly to spin-0  $Y_{\ell 2}$  spherical harmonic functions. This new notation also allows us to derive real space operators which decompose the measured Stokes parameters into their even and odd-parity parts, without ever evaluating the scalar  $E/B$  fields themselves. This paper is the first part in a series of papers that explore real-space computation of polarization modes and their applications.

---

## Contents

<b>1</b>	<b>Introduction</b>	<b>1</b>
<b>2</b>	<b>Polarization primer</b>	<b>2</b>
2.1	Constructing $E/B$ fields without harmonic space	2
2.2	Standard $E/B$ fields	3
<b>3</b>	<b>Real space polarization operators</b>	<b>4</b>
3.1	Matrix notation	4
3.2	Evaluating scalar $E/B$ from Stokes $Q/U$	6
3.3	Evaluating Stokes $Q/U$ from scalar $E/B$	9
3.4	Purifying Stokes parameters $Q/U$ from $E/B$ modes	9
3.5	Visualizing the real space kernels	12
3.6	The non-locality of the real space operators	13
3.6.1	Generalized operators	16
3.6.2	Recovering the default $E$ and $B$ mode spectra	18
3.6.3	Relation to the spin raising $\bar{\partial}^2$ and lowering $\bar{\partial}^2$ operators	18
<b>4</b>	<b>Discussion</b>	<b>20</b>

---

## 1 Introduction

The Cosmic Microwave Background is 10 percent polarized, but the polarization contains independent cosmological information.

Standard technique is to convert Stokes parameters into scalar and pseudo-scalar modes, which are easier to compare to theory.

The pseudo-scalar  $B$  mode is particularly important because it cannot be generated by primordial scalar perturbations

primordial tensor perturbations

lensing of  $E$ -modes

systematics checks

exotic phenomena like cosmic birefringence

The spin-0  $E/B$  modes relate to the spin-2 Stokes parameters via the spin-raising and -lowering operators ( $\bar{\partial}$ ,  $\bar{\partial}$ ), which are second derivatives evaluated locally. However, in practice we compute  $E/B$  modes to a specified band limit, and this makes them non-local functions of the polarization field. In other words, the  $E/B$  modes at a point can get contributions from all over the sky.

(stuff about foregrounds, masking, ambiguous modes with references)

Zaldarriaga explored the spatial real-space kernels in the flat-sky approximation [].

In this work we follow the convention in which bar-ed variables correspond to those in real space, while the tilde-ed variables correspond to those in harmonic space [1].

This paper is organized in the following manner: In Sec. ?? we present a primer on the description of CMB polarization on the sphere and introduce the matrix notation which provides a more concise description of the same. In Sec. ?? we introduce the necessary tools and discuss the derivations of the real space operators. In Sec. 3.5 we evaluate the real space

operators and present visualizations of these functions. Here we also discuss the locality of the real space E & B operators. In Sec. ?? we implement these operators to evaluate E & B maps from the Stokes parameters Q & U and compare these maps and their spectra from those derived using Healpix. We conclude with a discussion and the scope of this new method of analyzing CMB polarization in Sec. 4.

## 2 Polarization primer

### 2.1 Constructing $E/B$ fields without harmonic space

CMB polarization is measured in terms of Stokes parameters, time averages of the linear polarization of the electric field along cartesian axes perpendicular to the line of sight.<sup>1</sup> Thus Stokes  $Q$  and  $U$  depend on the choice of the local coordinate system, and a rotation by an angle  $\psi$  around the line of sight transforms them as

$$\begin{bmatrix} Q \\ U \end{bmatrix}' = \begin{bmatrix} \cos 2\phi & \sin 2\phi \\ -\sin 2\phi & \cos 2\phi \end{bmatrix} \begin{bmatrix} Q \\ U \end{bmatrix}. \quad (2.1)$$

Equivalently the object  ${}_{+2}\bar{X}(\hat{n}) = Q(\hat{n}) \pm iU(\hat{n})$  transforms as  ${}_{+2}f' = e^{\mp 2i\phi} {}_s f$  and hence forms a spin-2 field [2].

The standard construction of  $E$  and  $B$  fields arise from the desire to have a coordinate independent description of the polarization. This follows from operations that raise (or lower) the spin of the  $X$  field to construct scalar fields. But from the transform properties of the Stokes parameters, we can already construct a heuristic argument for what these operations must look like in real space.

We consider the contribution to a scalar field at  $\hat{n}_e$  from the polarization field at  $\hat{n}_q$ . Fig. 1 shows that the transformation of the local coordinate system between the two positions can be described by a rotation around the local  $\hat{n}_q$  by angle  $\alpha$ , parallel transport by angle  $\beta$ , and a rotation around  $\hat{n}_q$  by  $-\gamma$ . This corresponds to a rotation by Euler angles  $(\alpha, \beta, -\gamma)$  in the  $z - y_1 - z_2$  convention.<sup>2</sup>

Rotating the cartesian coordinates in the tangent plane at location  $\hat{n}_q$  by an angle  $\phi$  about the local  $\hat{z}_q$  axis, the Stokes parameters in the new coordinate system relate to those in the original coordinate system as:  $\mathcal{R}_{\hat{z}_q}(\phi)[{}_{+2}X(\hat{n}_q)] = {}_{+2}X(\hat{n}_q)e^{-i2\phi}$ . This same rotation by  $\phi$  alters the Euler angle  $\alpha_{qe}$  (that aligns the  $x$ -axis at  $\hat{n}_q$  along the geodesic to the location  $\hat{n}_e$ ):  $\mathcal{R}_{\hat{z}_q}(\phi)[\alpha_{qe}] = \alpha_{qe} - \phi$ . Therefore one can see that  $\mathcal{R}_{\hat{z}_q}(\phi)[e^{-i2\alpha_{qe}}] = e^{-i2\alpha_{qe}}e^{i2\phi}$ .

Given these transformation properties, the combination  ${}_{+2}X(\hat{n}_q)e^{-i2\alpha'_{qe}}$  is invariant under rotations and must be spin-0 by definition:

$$\mathcal{R}_{\hat{z}_q}(\phi)[{}_{+2}X(\hat{n}_q)e^{-i2\alpha'_{qe}}] = {}_{+2}X(\hat{n}_q)e^{-i2\alpha_{qe}} \quad (2.2)$$

The real part of the function is constructed by product of functions  $(Q \cos 2\alpha, U \sin 2\alpha)$  having the same parity and hence the real part must have even parity. At the same time, the imaginary part of the function is constructed by multiplying functions  $(Q \sin 2\alpha, U \cos 2\alpha)$  of opposite parity and hence must have an odd parity. Therefore we can make the association that contributions to  $(E + iB)(\hat{n}_e)$  must be proportional to  ${}_{+2}X(\hat{n}_q)e^{-i2\alpha_{qe}}$ .

---

<sup>1</sup>Throughout we use the conventions of HEALPix [?], measuring the polarization angle East of South.

<sup>2</sup>The Euler angles in the more standard  $z - y - z$  convention are related to those in the  $z - y_1 - z_2$  convention by the following rule:  $(\alpha, \beta, \gamma)_{z-y-z} = (\gamma, \beta, \alpha)_{z-y_1-z_2}$  [4].

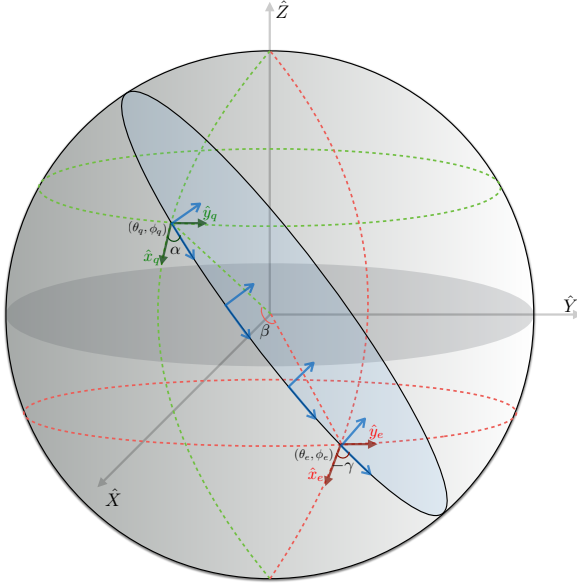


**Figure 1:** This figure depicts the Euler angles in the z-y1-z2 convention. The cartesian coordinates shown in dark green are those that lie in the tangent plane at location  $\hat{n}_q = (\theta_q, \phi_q)$  while those shown in dark red are the ones that lie in the tangent plane at location  $\hat{n}_e = (\theta_e, \phi_e)$ . The blue coordinates at different locations are representative of the parallel transport along the geodesic connection the two locations  $\hat{n}_q$  &  $\hat{n}_e$  on the sphere.

The same rotation  $\mathcal{R}_{\hat{z}_q}(\phi)$  leaves the Euler angle  $|\beta_{qe}|$  unaltered (it measures the angular distance between the points). Thus we can conclude that the contribution to  $(E + iB)(\hat{n}_e)$  from the position  $n_q$  must have the form

$$+_2 X(\hat{n}_q) f(\beta_{qe}) e^{-i2\alpha_{qe}} \quad (2.3)$$

for some real function  $f$ . Note that when the two locations coincide ( $\beta_{qe} = 0$ ) then  $\alpha_{qe} = 0, 2\pi, 4\pi, \dots$ , implying  $E + iB \propto Q + iU$ . This is a contradiction because  $Q + iU$  does not transform as a spin-0 field under local rotations, and so we must have  $f(\beta_{qe} = 0) = 0$ . Hence the  $E/B$  fields are necessarily non-local. A similar contradiction arises when the two locations are diametrically opposite,  $\beta_{qe} = \pi$ , and so  $f(\beta_{qe} = \pi) = 0$ . Any such function  $f$  will let us construct  $E/B$ -like scalar fields. Below we derive the particular one that gives rise to our familiar  $E/B$  modes.

This type of construction can be generalized to transform a field of any spin to a field of any other spin, not just two and zero, and so we can use a similar construction (in the opposite direction) to transform  $E/B$  maps back to the Stokes parameters (i.e. transforming spin-0 fields to spin-2).

## 2.2 Standard $E/B$ fields

The standard construction of  $E/B$  fields depend on the spin-raising and -lowering operators, and is usually carried out in harmonic space. The spin-raising operator ( $\bar{\partial}$ ), applied to a field of spin- $s$   ${}_s g$ , results in a fields with spin- $(s+1)$ :  $(\bar{\partial}_s g)' = e^{-i(s+1)\phi} (\bar{\partial}_s g)$  [3]. The complementary spin-lowering operator ( $\bar{\partial}$ ) similarly results with  $(\bar{\partial}_s g)' = e^{-i(s-1)\phi} (\bar{\partial}_s g)$ . The

complex spin-0 scalar now arise from the spin-2 fields  $\pm_2 X$  as follows,

$$\mathcal{E}(\hat{n}) + i\mathcal{B}(\hat{n}) = -\bar{\eth}_{+2}^2 \tilde{X}(\hat{n}), \quad (2.4a)$$

$$\mathcal{E}(\hat{n}) - i\mathcal{B}(\hat{n}) = -\bar{\eth}_{-2}^2 \tilde{X}(\hat{n}). \quad (2.4b)$$

The  $\mathcal{E}/\mathcal{B}$  fields are defined locally at point  $\hat{n}$  in terms of the derivative operators  $\eth$  and  $\bar{\eth}$ .

We can decompose the complex field  $\pm_2 X$  into spin spherical harmonic functions:  $\pm_2 X(\hat{n}) = \sum_{\ell m} \pm_2 X_{\ell m} \pm_2 Y_{\ell m}(\hat{n})$ . On applying the spin raising and lowering operators on the spin spherical harmonic functions leads to the following identities [3],

$$\eth_s Y_{\ell m}(\hat{n}) = \sqrt{(\ell - s)(\ell + s + 1)} {}_{s+1} Y_{\ell m}(\hat{n}), \quad (2.5a)$$

$$\bar{\eth}_s Y_{\ell m}(\hat{n}) = -\sqrt{(\ell + s)(\ell - s + 1)} {}_{s-1} Y_{\ell m}(\hat{n}), \quad (2.5b)$$

where  ${}_s Y_{\ell m}(\hat{n})$  denote the spin-s spherical harmonics.

From the definition of  $\mathcal{E}/\mathcal{B}$ , the spin spherical harmonic decomposition of  $\pm_2 X$ , and the identities given in Eq. (2.5), it follows that the scalar fields  $\mathcal{E}/\mathcal{B}$  are,

$$\mathcal{E}(\hat{n}) = \sum_{\ell m} a_{\ell m}^E \sqrt{\frac{(\ell + 2)!}{(\ell - 2)!}} Y_{\ell m}(\hat{n}); \quad \mathcal{B}(\hat{n}) = \sum_{\ell m} a_{\ell m}^B \sqrt{\frac{(\ell + 2)!}{(\ell - 2)!}} Y_{\ell m}(\hat{n}), \quad (2.6)$$

where the harmonic coefficients  $a_{\ell m}^E$  and  $a_{\ell m}^B$  relate to the harmonic coefficients of the spin-2 polarization field via,

$$a_{\ell m}^E = -\frac{1}{2} \left[ {}_{+2} \tilde{X}_{\ell m} + {}_{-2} \tilde{X}_{\ell m} \right]; \quad a_{\ell m}^B = -\frac{1}{2i} \left[ {}_{+2} \tilde{X}_{\ell m} - {}_{-2} \tilde{X}_{\ell m} \right]. \quad (2.7)$$

In the remainder of this article, we will work with the scalar  $E$  and pseudo scalar  $B$  fields, defined by:

$$E(\hat{n}) = \sum_{\ell m} a_{\ell m}^E Y_{\ell m}(\hat{n}); \quad B(\hat{n}) = \sum_{\ell m} a_{\ell m}^B Y_{\ell m}(\hat{n}). \quad (2.8)$$

These  $E/B$  fields are merely red-filtered versions of  $\mathcal{E}/\mathcal{B}$  (their spherical harmonic coefficients of expansion are related by the factor  $[(\ell + 2)!/(\ell - 2)!]^{1/2}$ ), and are not local functions of Stokes  $Q/U$ .

### 3 Real space polarization operators

#### 3.1 Matrix notation

Our derivation of real space operators is more transparent in a matrix-vector notation.<sup>3</sup> We introduce a matrix that encodes spin spherical harmonic basis vectors,

$$|s| \mathcal{Y} = \begin{bmatrix} {}_{+s} Y & 0 \\ 0 & {}_{-s} Y \end{bmatrix}_{2N_{\text{pix}} \times 2N_{\text{alms}}} \quad (3.1)$$

We will be working with cases  $s \in [0, 2]$ . Each column maps to a specific harmonic basis function (i.e. indexed by  $\ell m$ ) and each row maps to a pixel on the sphere. This matrix is

---

<sup>3</sup>While we work with the matrix and vector sizes given in terms of some pixelization parameter  $N_{\text{pix}}$ , all the relations are equally valid in the continuum limit attained by allowing  $N_{\text{pix}} \rightarrow \infty$

not square in general: the number of rows is determined by the pixelization and the number of columns is set by the number of basis functions (e.g. determined by the band limit).

We now define the different polarization data vectors and their representation in real space as and harmonic as follows,<sup>4</sup>

$$\bar{S} = \begin{bmatrix} E \\ B \end{bmatrix}_{2N_{\text{pix}} \times 1} ; \quad \bar{X} = \begin{bmatrix} {}^{+2}X \\ {}^{-2}X \end{bmatrix}_{2N_{\text{pix}} \times 1} ; \quad \bar{P} = \begin{bmatrix} Q \\ U \end{bmatrix}_{2N_{\text{pix}} \times 1}, \quad (3.2a)$$

$$\tilde{S} = \begin{bmatrix} a^E \\ a^B \end{bmatrix}_{2N_{\text{alms}} \times 1} ; \quad \tilde{X} = \begin{bmatrix} {}^{+2}\tilde{X} \\ {}^{-2}\tilde{X} \end{bmatrix}_{2N_{\text{alms}} \times 1}. \quad (3.2b)$$

The different symbols have the same meaning as that discussed in Sec. 2, except that the subscript  $\ell m$  for the spherical harmonic coefficients is suppressed for cleaner notation.

We define transformations between different representations of the polarization field (i.e. from  $Q, U$  to  $\pm_2 X$ ):

$$\bar{T} = \begin{bmatrix} \mathbb{1} & i\mathbb{1} \\ \mathbb{1} & -i\mathbb{1} \end{bmatrix}_{2N_{\text{pix}} \times 2N_{\text{pix}}} ; \quad \bar{T}^{-1} = \frac{1}{2}\bar{T}^\dagger, \quad (3.3a)$$

$$\tilde{T} = -\begin{bmatrix} \mathbb{1} & i\mathbb{1} \\ \mathbb{1} & -i\mathbb{1} \end{bmatrix}_{2N_{\text{alms}} \times 2N_{\text{alms}}} ; \quad \tilde{T}^{-1} = \frac{1}{2}\tilde{T}^\dagger, \quad (3.3b)$$

The sign conventions we have chosen match HEALPix. Using the data vectors and the matrix operators defined above we can now express, in compact notation, the forward and inverse relations between different representations of the polarization data vectors as follows,

$$\bar{X} = \bar{T}\bar{P}; \quad \bar{P} = \frac{1}{2}\bar{T}^\dagger\bar{X}; \quad (3.4a)$$

$$\tilde{X} = \tilde{T}\tilde{S}; \quad \tilde{S} = \frac{1}{2}\tilde{T}^\dagger\tilde{X}. \quad (3.4b)$$

Meanwhile the spherical harmonic transforms are written as:

$$\bar{X} = {}_2\mathcal{Y}\tilde{X}; \quad \tilde{X} = {}_2\mathcal{Y}^\dagger\bar{X}; \quad (3.4c)$$

$$\bar{S} = {}_0\mathcal{Y}\tilde{S}; \quad \tilde{S} = {}_0\mathcal{Y}^\dagger\bar{S}. \quad (3.4d)$$

Finally we introduce the operators that project harmonic space data vector to the  $E$  or  $B$  subspace,

$$\tilde{O}_E = \begin{bmatrix} \mathbb{1} & 0 \\ 0 & 0 \end{bmatrix}_{2N_{\text{alms}} \times 2N_{\text{alms}}} ; \quad \tilde{S}_E = \tilde{O}_E\tilde{S}, \quad (3.5a)$$

$$\tilde{O}_B = \begin{bmatrix} 0 & 0 \\ 0 & \mathbb{1} \end{bmatrix}_{2N_{\text{alms}} \times 2N_{\text{alms}}} ; \quad \tilde{S}_B = \tilde{O}_B\tilde{S}. \quad (3.5b)$$

Note that these harmonic space matrices are idempotent ( $\tilde{O}_E\tilde{O}_E = \tilde{O}_E$ ;  $\tilde{O}_B\tilde{O}_B = \tilde{O}_B$ ), orthogonal ( $\tilde{O}_E\tilde{O}_B = \emptyset$ ), and sum to the identity matrix ( $\tilde{O}_E + \tilde{O}_B = \mathbb{1}$ ). The above relations for these harmonic space operators are exactly valid. In the following sections we aim to derive the real space analogues ( $O_E, O_B$ ) of these harmonic space operators.

---

<sup>4</sup>We adopt a convention in which real space quantities are denoted by bar-ed variable while those in harmonic space are denoted by tilde-ed variables.

### 3.2 Evaluating scalar $E/B$ from Stokes $Q/U$

In Sec. 2 we described the conventional procedure of computing the scalar fields  $E/B$  from the Stokes parameters  $Q/U$ . In this section we derive the real space convolution kernels on the sphere which can be used to directly evaluate the scalar fields  $E & B$  on the sphere. We use the vector-matrix notation introduced in Sec. 3.1 to write down an operator equation relating the real space vector of scalars  $\bar{S}$  to the Stokes polarization vector  $\bar{P}$ ,

$$\bar{S} = {}_0\mathcal{Y}\tilde{T}^{-1}{}_2\mathcal{Y}^\dagger \bar{T}\bar{P} = \frac{1}{2}{}_0\mathcal{Y}\tilde{T}^\dagger{}_2\mathcal{Y}^\dagger \bar{T}\bar{P} \quad (3.6a)$$

$$= \bar{O}\bar{P}. \quad (3.6b)$$

The explicit form of the real space operator  $\bar{O}$  can be derived by contracting over all the matrix operators. This procedure is explicitly worked out in the following set of equations,

$$\bar{O} = \frac{1}{2}{}_0\mathcal{Y}\tilde{T}^\dagger{}_2\mathcal{Y}^\dagger \bar{T}, \quad (3.7a)$$

$$= -0.5 \begin{bmatrix} {}_0Y_e & 0 \\ 0 & {}_0Y_e \end{bmatrix} \begin{bmatrix} \mathbb{1} & \mathbb{1} \\ -i\mathbb{1} & i\mathbb{1} \end{bmatrix} \begin{bmatrix} {}_{+2}Y_q^\dagger & 0 \\ 0 & {}_{-2}Y_q^\dagger \end{bmatrix} \begin{bmatrix} \mathbb{1} & i\mathbb{1} \\ \mathbb{1} & -i\mathbb{1} \end{bmatrix}, \quad (3.7b)$$

$$= -0.5 \begin{bmatrix} \sum({}_0Y_e {}_2Y_q^\dagger + {}_0Y_e {}_{-2}Y_q^\dagger) & i\sum({}_0Y_e {}_2Y_q^\dagger - {}_0Y_e {}_{-2}Y_q^\dagger) \\ -i\sum({}_0Y_e {}_2Y_q^\dagger - {}_0Y_e {}_{-2}Y_q^\dagger) & \sum({}_0Y_e {}_2Y_q^\dagger + {}_0Y_e {}_{-2}Y_q^\dagger) \end{bmatrix}, \quad (3.7c)$$

where the symbol  ${}_0Y_e$  is used to denote the sub-matrix  ${}_0Y_{\hat{n}_e \times \ell m} \equiv {}_0Y_{\ell m}(\hat{n}_e)$ , the symbol  ${}_{\pm 2}Y_q^\dagger$  is used to denote the transposed conjugated matrix  ${}_{\pm 2}Y_{\ell m \times \hat{n}_q}^* \equiv {}_{\pm 2}Y_{\ell m}^*(\hat{n}_q)$  and the summation is over the multipole indices  $\ell, m$ . As before, we use the notation that the index  $e$  denotes the location where the scalar fields are being evaluated, and the index  $q$  denotes the location from which the Stokes parameters are being accessed. Using the conjugation properties of the spin spherical harmonic functions it can be shown that the following identity holds true,

$$\left[ \sum_{\ell m} {}_0Y_{\ell m}(\hat{n}_e) {}_{+2}Y_{\ell m}^*(\hat{n}_q) \right]^* = \sum_{\ell m} {}_0Y_{\ell m}(\hat{n}_e) {}_{-2}Y_{\ell m}^*(\hat{n}_q), \quad (3.8)$$

where the terms on either side of the equation are those that appear in Eq. (3.7c). Note that the operator  $\bar{O}$  is real as one expects, since each sub-matrix in Eq. (3.7c) is formed by summing a complex number and its conjugate.

Eq. (3.7c) already presents a real space operator, but it is not in a form which can be practically implemented. To proceed, we use the fact that the  $m$  sum over the product of two spin spherical harmonic functions can be expressed as a function of the Euler angles [4],

$$\sum_m {}_{s_1}Y_{\ell m}^*(\hat{n}_i) {}_{s_2}Y_{\ell m}(\hat{n}_j) = \sqrt{\frac{2\ell+1}{4\pi}} {}_{s_2}Y_{\ell-s_1}(\beta_{ij}, \alpha_{ij}) e^{-is_2\gamma_{ij}}, \quad (3.9)$$

where  $\alpha_{ij}$ ,  $\beta_{ij}$  &  $\gamma_{ij}$  denote the Euler angles that specifically transform  $(i \rightarrow j)$ : the coordinate system at  $\hat{n}_i$  to align the coordinate system at  $\hat{n}_j$ <sup>5</sup>.

---

<sup>5</sup>The sense of the rotation become more obvious when this equation is written in terms of the Wigner-D functions.

Using this identity, the different parts of the real space operator  $\bar{O}$  (from eq. 3.7c) are completely specified by the complex function,

$$\begin{aligned}\mathcal{M}(\hat{n}_e, \hat{n}_q) &= \mathcal{M}_r + i\mathcal{M}_i, \\ &= \sum_{\ell m} {}_0Y_{\ell m}(\hat{n}_e) - {}_2Y_{\ell m}^*(\hat{n}_q) = \sum_{\ell} \sqrt{\frac{2\ell+1}{4\pi}} {}_0Y_{\ell 2}(\beta_{qe}, \alpha_{qe}),\end{aligned}\quad (3.10a)$$

$$= \left[ \cos(2\alpha_{qe}) + i \sin(2\alpha_{qe}) \right] \sum_{\ell=\ell_{\min}}^{\ell_{\max}} \frac{2\ell+1}{4\pi} \sqrt{\frac{(\ell-2)!}{(\ell+2)!}} P_{\ell 2}(\cos \beta_{qe}), \quad (3.10b)$$

$$= \left[ \cos(2\alpha_{qe}) + i \sin(2\alpha_{qe}) \right] \mathcal{M}f(\beta_{qe}, \ell_{\min}, \ell_{\max}), \quad (3.10c)$$

where we have used the identity in Eq. (3.9) to simplify the product of the spherical harmonic functions. Note that the function depends only on two out of the three Euler angles. The azimuthal part depends only on the Euler angle  $\alpha_{qe}$ , and so its harmonic transform has no multipole  $\ell$  dependence. The azimuthal part is the crucial operation that translates between different spin representation of CMB polarization. Only the radial part  $f(\beta_{qe})$  depends only on the angular separation between locations and hence completely incorporates all the multipole  $\ell$  dependence.

Employing Eq. (3.10) to simplify the product of spherical harmonic functions in Eq. (3.7c), the real space operator  $\bar{O}$  can now be cast in this more useful form,

$$\bar{O} = - \begin{bmatrix} \mathcal{M}_r & \mathcal{M}_i \\ -\mathcal{M}_i & \mathcal{M}_r \end{bmatrix}_{2N_{\text{pix}} \times 2N_{\text{pix}}} = -\mathcal{M}f(\beta_{qe}, \ell_{\min}, \ell_{\max}) \begin{bmatrix} \cos(2\alpha_{qe}) & \sin(2\alpha_{qe}) \\ -\sin(2\alpha_{qe}) & \cos(2\alpha_{qe}) \end{bmatrix}, \quad (3.11)$$

where  $(\alpha_{qe}, \beta_{qe}, \gamma_{qe})$  denote the Euler angles which rotate the local cartesian system at  $\hat{n}_q$  (location where Stokes parameters are accessed) to the cartesian system at  $\hat{n}_e$  (location where the scalar fields are evaluated):  $\mathcal{R}(\alpha_{qe}, \beta_{qe}, \gamma_{qe})[\hat{n}_q] = \hat{n}_e$ .

**Radiating kernel.** The expression we call the *radiating kernel* allows us, like a Green's function, to evaluate the  $E/B$  field contribution due to a single Stoke parameter "charge" at a fixed location. The total  $E/B$  maps can then be thought of as the superposed radiation emerging from Stokes charges across the sphere. In this picture, we are effectively in the frame of the Stokes charge  ${}_{\pm 2}X$  and evaluate its contribution to the complex spin-0 scalar field  $E + iB$  across the sphere.

The  $E/B$  contribution from the Stokes parameters at some location  $\hat{n}_q$  is given by the following expression (Eq. (3.11) and Eq. (3.6b)),

$$\bar{S}_q(\hat{n}_e) = \begin{bmatrix} E_q \\ B_q \end{bmatrix}_q = -\mathcal{M}f(\beta_{qe}, \ell_{\min}, \ell_{\max}) \begin{bmatrix} \cos(2\alpha_{qe}) & \sin(2\alpha_{qe}) \\ -\sin(2\alpha_{qe}) & \cos(2\alpha_{qe}) \end{bmatrix} \begin{bmatrix} Q_q \\ U_q \end{bmatrix} \Delta\Omega. \quad (3.12)$$

The total map can be simply evaluated by summing over the contribution from the Stokes parameters at each location  $\hat{n}_q$ :  $\bar{S} = \sum_{q=1}^{N_{\text{pix}}} \bar{S}_q$ . This operation can be cast concisely as,

$$[E + iB](\hat{n}_e) = -\Delta\Omega \sum_{q=1}^{N_{\text{pix}}} [{}_{+2}X(\hat{n}_q) e^{-i2\alpha_{qe}}] \mathcal{M}f(\beta_{qe}), \quad (3.13a)$$

$$= \sum_{q=1}^{N_{\text{pix}}} {}_{+2}X(\hat{n}_q) \mathcal{M}_G(\hat{n}_q), \quad (3.13b)$$

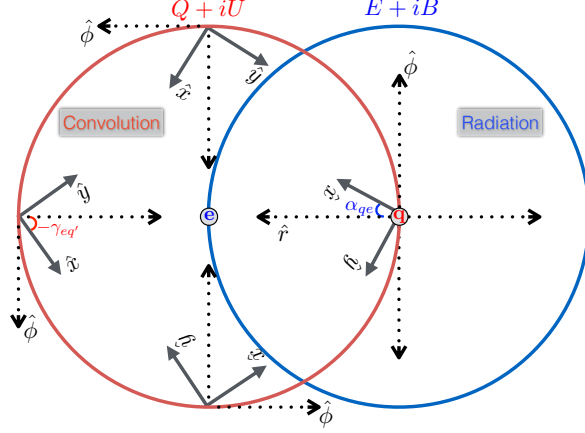


**Figure 2:** The local cartesian coordinate are only drawn on the red circle, representative of the coordinate dependence of the Stokes parameters. The value of the scalar field at location ‘e’ can be evaluated by summing over the contribution from all the Stokes parameters on the red circle (sphere). The convolutions are performed with kernels which are defined in term of the Euler angle  $\gamma_{eq}$ . Alternatively, one can compute the contribution from the Stokes parameter at location ‘q’ to all the point on the blue circle(sphere) and this is a function of the Euler angle  $\alpha_{eq}$ . In the flat sky limit, since  $\gamma = -\alpha$  there is no difference between the radiating and convolving kernels.

where the last line is a simple scalar multiplication between complex numbers. The radiating kernel is then:

$$\mathcal{M}_G(\hat{n}_e) = -\Delta\Omega \mathcal{M}^*(\beta_{qe}, \ell_{\min}, \ell_{\max}) e^{-i2\alpha_{qe}} \quad (3.14)$$

is  $-\Delta\Omega \mathcal{M}^*$  and can be thought of as the Green’s function of the operator. That is,  $[E + iB](\hat{n}_e) = \mathcal{M}_G$  is the spin-0 scalar field generated from the delta-function Stokes field  $[Q + iU](\hat{n}) = [\delta(\hat{n} - \hat{n}_q) + i0]$ .

**Convolution kernel.** We can also formulate the real space operator as a convolution operation, where the scalar field at  $\hat{n}_e$  gathers contributions from the Stokes fields. This is based around the inverse rotation from the previous section (to align the coordinate system at  $\hat{n}_e$  with that at  $\hat{n}_q$ ). The inverse rotation Euler angles relates to the forward rotation Euler angles by the following relations:  $\alpha_{eq} = -\gamma_{qe}$ ,  $\beta_{eq} = -\beta_{qe}$  and  $\gamma_{eq} = -\alpha_{qe}$ . Since the kernel only depends on the cosine of the Euler angle  $\beta$ , it is immune to changes in its sign. The operator equation can be expressed as a function of the Euler angle  $\gamma_{eq}$  as follows,

$$\begin{bmatrix} E_e \\ B_e \end{bmatrix} = - \sum_{q=1}^{N_{\text{pix}}} \mathcal{M} f(\beta_{eq}, \ell_{\min}, \ell_{\max}) \begin{bmatrix} \cos(2\gamma_{eq}) & -\sin(2\gamma_{eq}) \\ \sin(2\gamma_{eq}) & \cos(2\gamma_{eq}) \end{bmatrix} \begin{bmatrix} Q_q \\ U_q \end{bmatrix} \Delta\Omega, \quad (3.15)$$

This version of the real space operator would have naturally emerged had we simplified the the equivalent function  $\sum_{\ell m} 0Y_{\ell m}^*(\hat{n}_e) + 2Y_{\ell m}(\hat{n}_q)$  in Eq. (3.10). This formulation of the real space operator can be interpreted as integrating at some fixed location  $\hat{n}_e$  the  $E/B$  mode contribution arising from the Stokes parameters at all location  $\hat{n}_q$  on the sphere. This

operation can be expressed more concisely as follows,

$$[E + iB](\hat{n}_e) = -\Delta\Omega \sum_{q=1}^{N_{\text{pix}}} \left( \sum_{\ell=\ell_{\min}}^{\ell_{\max}} \frac{2\ell+1}{4\pi} \sqrt{\frac{(\ell-2)!}{(\ell+2)!}} P_\ell^2(\beta_{eq}) \right) \left( e^{i2\gamma_{eq}} {}_{+2}X(\hat{n}_q) \right), \quad (3.16a)$$

$$= \left\{ \left[ -\Delta\Omega \sum_{\ell=\ell_{\min}}^{\ell_{\max}} \sqrt{\frac{2\ell+1}{4\pi}} Y_{\ell 2}(\beta_{eq}, \gamma_{eq}) \right] \star {}_{+2}X \right\}(\hat{n}_e), \quad (3.16b)$$

$$= \left\{ \mathcal{M}_B \star {}_{+2}X \right\}(\hat{n}_e), \quad (3.16c)$$

where  $\star$  denotes a convolution and  $\mathcal{M}_B$  is merely the conjugated function  $\mathcal{M}^*$  when expressed as a function of the Euler angle  $\gamma_{eq}$  it can be thought of as an effective instrument beam pointing to the direction  $\hat{n}_e$ .

### 3.3 Evaluating Stokes $Q/U$ from scalar $E/B$

The real space operator which translates  $E$  &  $B$  fields to Stokes parameters  $Q$  &  $U$  can be derived using a similar procedure. Expressed in the matrix-vector notation, inverse operator is given by,

$$\bar{P} = \bar{T}^{-1} {}_2\mathcal{Y} \tilde{T}_0 \mathcal{Y}^\dagger \bar{S} = \frac{1}{2} \bar{T}^\dagger {}_2\mathcal{Y} \tilde{T}_0 \mathcal{Y}^\dagger \bar{S}, \quad (3.17a)$$

$$= \bar{O}^{-1} \bar{S}. \quad (3.17b)$$

The inverse operator expressed in terms of the function  $\mathcal{M}$  given in Eq. (3.10) is given by the following equation,

$$\bar{O}^{-1} = - \begin{bmatrix} \mathcal{M}_r & -\mathcal{M}_i \\ \mathcal{M}_i & \mathcal{M}_r \end{bmatrix}_{2N_{\text{pix}} \times 2N_{\text{pix}}} = -\mathcal{M}f(\beta_{eq}, \ell_{\min}, \ell_{\max}) \begin{bmatrix} \cos(2\alpha_{qe}) & -\sin(2\alpha_{qe}) \\ \sin(2\alpha_{qe}) & \cos(2\alpha_{qe}) \end{bmatrix}, \quad (3.18)$$

where all the symbols have the same meaning as discussed in Sec. 3.2. Note that the kernel in the above equation differs from the one in Eq. (3.11) by a change in sign on the off-diagonals of the block matrix. When expressed in terms of the same set of Euler angles used to define the operator  $\bar{O}$ , it can be shown that the different forms of the real space operator are given by,

$${}_{+2}X(\hat{n}_q) = \sum_{e=1}^{N_{\text{pix}}} [E + iB](\hat{n}_e) \mathcal{M}_B^*[\hat{n}_e] \quad \text{Radiation kernel} \quad (3.19)$$

$${}_{+2}X(\hat{n}_q) = \left\{ \mathcal{M}_G^* \star [E + iB] \right\}(\hat{n}_q) \quad \text{Convolution kernel}, \quad (3.20)$$

where all the symbols have the same meaning as defined in Sec. 3.2. Note that the conjugated forms of the Green's function and the effective beam for the operator  $\bar{O}$  have their roles reversed for the inverse operator  $\bar{O}^{-1}$ .

### 3.4 Purifying Stokes parameters $Q/U$ from $E/B$ modes

We can only measure the total Stokes vector, a sum of the part corresponding to scalar  $E$  and the part corresponding to  $B$ . The  $E/B$  modes are orthogonal to each other in the

sense that their respective operators are orthogonal to each other as seen in Eq. (??). It is possible to decompose the Stokes vector  $\bar{P}$  into one  $\bar{P}_E$  that purely contributes to  $E$  modes and another  $\bar{P}_B$  that purely contribute to the  $B$  modes of polarization. In this section we derive the real space operators which operate on the total Stokes vector and yield this decomposition, without ever having to explicitly evaluate the scalar modes. The algebra is more involved, but the derivation is similar to that discussed in Sec. 3.2, so we refrain from presenting the detailed calculations here, and outline only the key points. We use the harmonic space projection operators  $\tilde{O}_{E/B}$ , defined in Eq. (3.5), to derive the respective real space operators. The Stokes parameters corresponding to each scalar mode are given by the following expressions,

$$\begin{aligned}\bar{P}_E &= [\bar{T}^{-1} {}_2\mathcal{Y} \tilde{T} \tilde{O}_E \tilde{T}^{-1} * {}_2\mathcal{Y}^\dagger \bar{T}] \bar{P}, \\ &= [\frac{1}{4} \bar{T}^\dagger {}_2\mathcal{Y} \tilde{T} \tilde{O}_E \tilde{T}^\dagger {}_2\mathcal{Y}^\dagger \bar{T}] \bar{P}, \\ &= \bar{O}_E \bar{P},\end{aligned}\tag{3.21}$$

$$\begin{aligned}\bar{P}_B &= [\bar{T}^{-1} {}_2\mathcal{Y} \tilde{T} \tilde{O}_B \tilde{T}^{-1} {}_2\mathcal{Y}^\dagger \bar{T}] \bar{P}, \\ &= [\frac{1}{4} \bar{T}^\dagger {}_2\mathcal{Y} \tilde{T} \tilde{O}_B \tilde{T}^\dagger {}_2\mathcal{Y}^\dagger \bar{T}] \bar{P}, \\ &= \bar{O}_B \bar{P}.\end{aligned}\tag{3.22}$$

We contract over all the matrix operators to arrive at the the real space operators. On working through the algebra it can be shown that the real space operators have the following form,

$$\bar{O}_{E/B} = 0.5 \begin{bmatrix} \mathcal{I}_r & \mathcal{I}_i \\ -\mathcal{I}_i & \mathcal{I}_r \end{bmatrix} \pm 0.5 \begin{bmatrix} \mathcal{D}_r & \mathcal{D}_i \\ \mathcal{D}_i & -\mathcal{D}_r \end{bmatrix},\tag{3.23}$$

where  $\mathcal{I}_r$  &  $\mathcal{D}_r$  and  $\mathcal{I}_i$  &  $\mathcal{D}_i$  are the real and complex parts of the following complex functions,

$$\mathcal{I}(\hat{n}_e, \hat{n}_q) = \mathcal{I}_r + i\mathcal{I}_i = \sum_{\ell m} {}_{-2}Y_{\ell m}(\hat{n}_e) {}_{-2}Y_{\ell m}^*(\hat{n}_q),\tag{3.24a}$$

$$\mathcal{D}(\hat{n}_e, \hat{n}_q) = \mathcal{D}_r + i\mathcal{D}_i = \sum_{\ell m} {}_2Y_{\ell m}(\hat{n}_e) {}_{-2}Y_{\ell m}^*(\hat{n}_q).\tag{3.24b}$$

These functions can be further simplified using the identity of spin spherical harmonics given in Eq. (3.9). Specifically it can be shown that these functions reduce to the following mathematical forms,

$$\mathcal{I}(\hat{n}_e, \hat{n}_q) = \sum_{\ell} \sqrt{\frac{2\ell+1}{4\pi}} {}_{-2}Y_{\ell 2}(\beta_{qe}, \alpha_{qe}) e^{i2\gamma_{qe}} = \mathcal{I}_r + i\mathcal{I}_i,\tag{3.25a}$$

$$\mathcal{I}_r + i\mathcal{I}_i = [\cos(2\alpha_{qe} + 2\gamma_{qe}) + i \sin(2\alpha_{qe} + 2\gamma_{qe})] \mathcal{I}f(\beta_{qe}, \ell_{\min}, \ell_{\max}),\tag{3.25b}$$

$$\mathcal{D}(\hat{n}_q, \hat{n}_e) = \sum_{\ell} \sqrt{\frac{2\ell+1}{4\pi}} {}_2Y_{\ell 2}(\beta_{qe}, \alpha_{qe}) e^{-i2\gamma_{qe}} = \mathcal{D}_r + i\mathcal{D}_i,\tag{3.26a}$$

$$\mathcal{D}_r + i\mathcal{D}_i = [\cos(2\alpha_{qe} - 2\gamma_{qe}) + i \sin(2\alpha_{qe} - 2\gamma_{qe})] \mathcal{D}f(\beta_{qe}, \ell_{\min}, \ell_{\max}),\tag{3.26b}$$

where the radial functions are given by,

$${}_{\mathcal{D}/\mathcal{I}} f(\beta, \ell_{\min}, \ell_{\max}) = \sum_{\ell=\ell_{\min}}^{\ell_{\max}} \sqrt{\frac{2\ell+1}{4\pi}} {}_{\mathcal{D}/\mathcal{I}} f_{\ell}(\beta), \quad (3.27)$$

where the functions  $\pm {}_2 f_{\ell}(\beta)$  Is the prescript correct? are expressed in terms of  $P_{\ell}^2$  Legendre polynomials and are given by the following explicit mathematical forms,

$$\begin{aligned} {}_{\mathcal{D}/\mathcal{I}} f_{\ell}(\beta) &= 2 \frac{(\ell-2)!}{(\ell+2)!} \sqrt{\frac{2\ell+1}{4\pi}} \left[ -P_{\ell}^2(\cos \beta) \left( \frac{\ell-4}{\sin^2 \beta} + \frac{1}{2} \ell(\ell-1) \pm \frac{2(\ell-1) \cos \beta}{\sin^2 \beta} \right) \right. \\ &\quad \left. + P_{\ell-1}^2(\cos \beta) \left( (\ell+2) \frac{\cos \beta}{\sin^2 \beta} \pm \frac{2(\ell+2)}{\sin^2 \beta} \right) \right]. \end{aligned} \quad (3.28)$$

Finally the Stokes parameters corresponding to the respective scalar fields can be computed by evaluating the following expressions,

$$\begin{aligned} \begin{bmatrix} Q_e \\ U_e \end{bmatrix}_{E/B} &= \sum_{q=1}^{N_{\text{pix}}} \left\{ {}_{\mathcal{I}} f(\beta_{qe}, \ell_{\min}, \ell_{\max}) \begin{bmatrix} \cos(2\alpha_{qe} + 2\gamma_{qe}) & \sin(2\alpha_{qe} + 2\gamma_{qe}) \\ -\sin(2\alpha_{qe} + 2\gamma_{qe}) & \cos(2\alpha_{qe} + 2\gamma_{qe}) \end{bmatrix} \begin{bmatrix} Q_q \\ U_q \end{bmatrix} \right. \\ &\quad \left. \pm {}_{\mathcal{D}} f(\beta_{qe}, \ell_{\min}, \ell_{\max}) \begin{bmatrix} \cos(2\alpha_{qe} - 2\gamma_{qe}) & \sin(2\alpha_{qe} - 2\gamma_{qe}) \\ \sin(2\alpha_{qe} - 2\gamma_{qe}) & -\cos(2\alpha_{qe} - 2\gamma_{qe}) \end{bmatrix} \begin{bmatrix} Q_q \\ U_q \end{bmatrix} \right\} \frac{\Delta\Omega}{2}, \end{aligned} \quad (3.29)$$

where all the symbols have their usual meaning. The above expression can be cast in the further simplified form,

$$\begin{aligned} {}_{+2} X_{E/B}(\hat{n}_e) &= 0.5 \Delta\Omega \sum_{q=1}^{N_{\text{pix}}} {}_{\mathcal{I}} f(\beta_{qe}) e^{-i2(\alpha_{qe} + \gamma_{qe})} {}_{+2} X(\hat{n}_q) \pm {}_{\mathcal{D}} f(\beta_{qe}) e^{i2(\alpha_{qe} - \gamma_{qe})} {}_{+2} X(\hat{n}_q)^*, \\ &= 0.5 \left\{ {}_{+2} X \mathcal{I}_G^* \pm {}_{+2} X^* \mathcal{D}_G \right\} \quad \text{Radiation kernel}, \end{aligned} \quad (3.30a)$$

$$= 0.5 \left\{ \mathcal{I}_B * {}_{+2} X \pm \mathcal{D}_B * {}_{+2} X^* \right\} \quad \text{Convolution kernel}, \quad (3.30b)$$

where all the symbols have their usual meaning and the explicit multipole dependence of the real space operators has been suppressed for brevity. Note that when the operators  $\mathcal{I}^*$  and  $\mathcal{D}$  are expressed in terms of the Euler angles  $(\alpha_{qe}, \beta_{qe}, \gamma_{qe})$  they can be interpreted as the Greens functions and we denote them as  $\mathcal{I}_G^*$  and  $\mathcal{D}_G$ . When expressed as function of Euler angles  $(\alpha_{eq}, \beta_{eq}, \gamma_{eq})$  corresponding to the inverse rotations they can be interpreted as a some convolving beam and we denote them as  $\mathcal{I}_B$  and  $\mathcal{D}_B$ . Note that unlike in the case of the operators  $\mathcal{M}_G$  and  $\mathcal{M}_B$  which have different shapes owing to their dependence on Euler angles  $\alpha$  and  $\gamma$  respectively, the operators  $\mathcal{D}_G$  and  $\mathcal{D}_B$  are identical since  $(\alpha_{qe} - \gamma_{qe}) = (\alpha_{eq} - \gamma_{eq})$ , while  $\mathcal{I}_G^*$  and  $\mathcal{I}_B$  are related by conjugation since  $(\alpha_{qe} + \gamma_{qe}) = -(\alpha_{eq} + \gamma_{eq})$ .

The operator  $\mathcal{I}$  is Hermitian and is a band limited version of the delta function owing to the identity  $\lim_{\ell \rightarrow \infty} \mathcal{I} = \delta(\hat{n}_i - \hat{n}_j)$ . For all practical purposes  $\mathcal{I}$  acts like an identity operator as is confirmed by the following set of identities: (i)  $\mathcal{I}\mathcal{I} = \mathcal{I}$ ; (ii)  $\mathcal{D}\mathcal{I} = \mathcal{D}$ .  $\mathcal{D}$  is a complex but symmetric matrix and  $\mathcal{D}^*$  is its inverse in this band limited sense:  $\mathcal{D}^*\mathcal{D} = \mathcal{I}$ . Using these

properties of the operators  $\mathcal{I}$  and  $\mathcal{D}$ , one can verify that the real space operators satisfy the following identities,

$$\bar{O}_E \bar{O}_E = \bar{O}_E; \quad \bar{O}_B * \bar{O}_B = \bar{O}_B, \quad (3.31a)$$

$$\bar{O}_E \bar{O}_B = 0, \quad (3.31b)$$

$$\bar{O}_E + \bar{O}_B = \mathcal{I}, \quad (3.31c)$$

which are the real space analogues of Eq. (??).<sup>6</sup>

Note that unlike in the harmonic case, the sum of the operators is the band limited identity operator  $\mathcal{I}$ . This non-exactness is representative of the loss of information resulting from making this transformation on the measured data with some imposed band limit. Forcing the sum of the operators to be exactly an identity matrix compromises the orthogonality property of the  $\bar{O}_E$  &  $\bar{O}_B$  operators which is exact and a more crucial property of the operators.

### 3.5 Visualizing the real space kernels

We compute the Euler angles  $(\alpha, \beta, \gamma)$  given the angular coordinates of any two Healpix pixels and use these to evaluate the convolution and radiation kernels. To provide an intuition for how these kernels vary as a function of position of the central pixel we depict in Fig. 3 the respective kernels at a few different locations on the sphere. While the kernels are evaluated in the band limit  $\ell \in [2, 192]$ , for illustration these functions are sampled at a very high Healpix resolution parameter of NSIDE=2048. All the plots have been rotated such that the central location marked by the black circle are in the centre of the figure. The horizontal and vertical lines that pass through the central black circle mark the local latitude and longitude respectively.

The real and imaginary part of the kernel  $\mathcal{M}_G$  are identical irrespective of changes in the galactic latitude and longitude of the central pixel. This is consistent with the Green's function interpretation of these kernels. Note that these functions are not distorted when a part of the domain overlaps with the poles, as can be seen in the first three rows of Fig. 3. Both these facts can be associated with the fact that this function does not depend on the Euler angle  $\gamma$ . From Eq. (3.15) and Eq. (??) it is clear that  $\mathcal{M}_r$  and  $\mathcal{M}_i$  can be interpreted in the following ways,

$$\begin{bmatrix} E = \text{Re}(\mathcal{M}_G) \\ B = \text{Im}(\mathcal{M}_G) \end{bmatrix} \leftarrow \begin{bmatrix} Q = \delta(\hat{n} - \hat{n}_q) \\ U = 0 \end{bmatrix}; \quad \begin{bmatrix} E = -\text{Im}(\mathcal{M}_G) \\ B = +\text{Re}(\mathcal{M}_G) \end{bmatrix} \leftarrow \begin{bmatrix} Q = 0 \\ U = \delta(\hat{n} - \hat{n}_q) \end{bmatrix}, \quad (3.32a)$$

$$\begin{bmatrix} Q = \text{Re}(\mathcal{M}_B^*) \\ U = \text{Im}(\mathcal{M}_B^*) \end{bmatrix} \leftarrow \begin{bmatrix} E = \delta(\hat{n} - \hat{n}_e) \\ B = 0 \end{bmatrix}; \quad \begin{bmatrix} Q = -\text{Im}(\mathcal{M}_B^*) \\ U = \text{Re}(\mathcal{M}_B^*) \end{bmatrix} \leftarrow \begin{bmatrix} E = 0 \\ B = \delta(\hat{n} - \hat{n}_e) \end{bmatrix}. \quad (3.32b)$$

The kernels  $\mathcal{D}$  &  $\mathcal{I}$  vary significantly as a function of galactic latitude of the central pixel as seen in the last four columns of Fig. 3. These kernels show a two fold symmetry in the vicinity of the poles and this arises due to Euler angle  $\gamma \approx 0$  here and therefore  $e^{i2(\alpha \pm \gamma)} \approx e^{i2\alpha}$ . Note that in this region, the azimuthal profile of the real and imaginary part of these kernels is similar to  $\mathcal{M}_r$  and  $\mathcal{M}_i$  respectively. This explains why the imaginary part of the band limited delta function  $\mathcal{I}$  contributes just as much as the real part in these regions. On transiting to lower latitudes,  $\mathcal{D}$  quickly transitions to having a four fold symmetry while  $\mathcal{I}$  transitions

---

<sup>6</sup>While testing the above stated identities one encounters terms like  $\mathcal{D}\mathcal{I}^*$ ,  $\mathcal{I}^*\mathcal{I}$  and  $\mathcal{I}\mathcal{I}^*$  which cannot be simply interpreted but they always occur in pairs with opposite signs that exactly cancel each other.

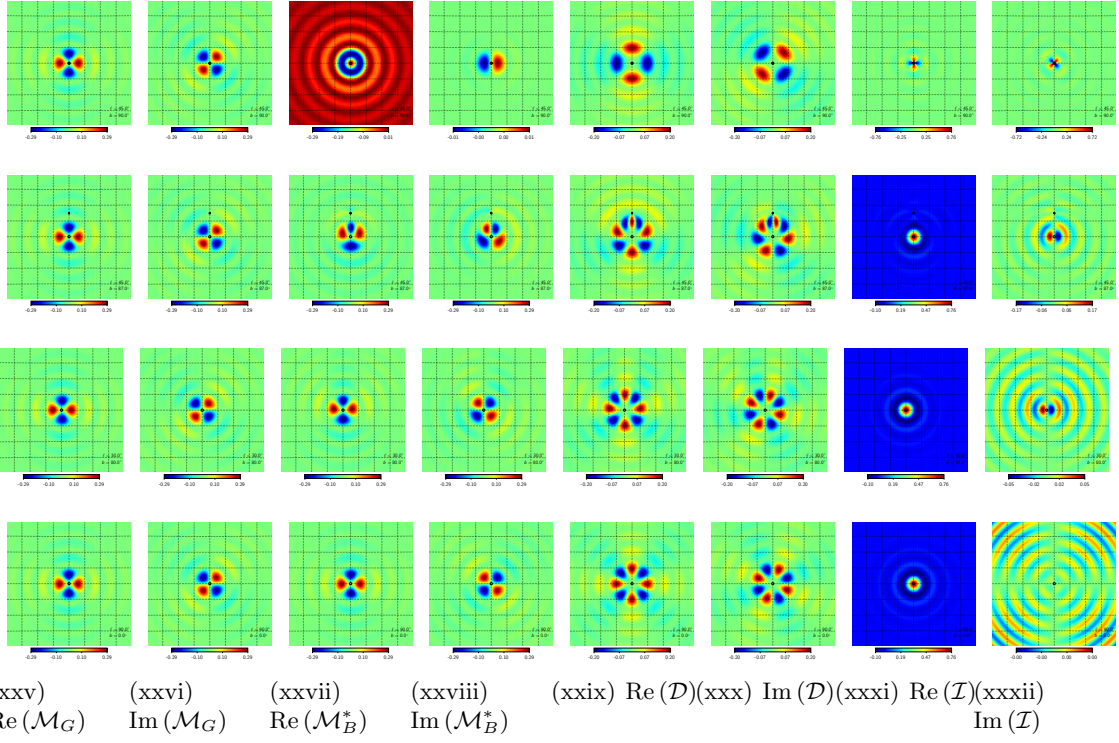


**Figure 3:** This panel of figure depicts the real and imaginary parts of the real space kernels  $\mathcal{M}_G$ ,  $\mathcal{M}_B$ ,  $\mathcal{D}$  &  $\mathcal{I}$  respectively. These kernels have been evaluated with the band limit:  $\ell \in [2, 192]$  and sampled at the Healpix resolution parameter NSIDE=2048 for visual appeal. The size of each panel is approximately  $16^\circ \times 16^\circ$  and the grid lines are marked at 2 degree separations. The black circles denotes the position of the center around which the kernels have been evaluated while the black star marks the location of the north galactic pole. The four rows depict the kernels at different location on the sphere and the galactic coordinates of the central pixel are specified in each panel.

to being dominated by the real part and behaves more like the conventional delta function. This transition can be most easily understood in the flat sky limit where  $\gamma = -\alpha$  which leads to the resultant 4 fold symmetry seen for  $\mathcal{D}$  owing to  $e^{i2(\alpha-\gamma)} = e^{i4\alpha}$  and  $\mathcal{I}$  being dominated by the real part owing to  $e^{-i2(\alpha+\gamma)} = 1 + i0$ . Since the flat sky approximation has most validity in the proximity of the equator these limiting tendencies of the respective kernels are seen in the bottom row of Fig. 3 which depict the kernels evaluated at the equator  $b = 0^\circ$ . The middle two row depict the kernels evaluated at a latitudes of  $b = 87^\circ$  &  $80^\circ$  and serve to indicate the rate of this transition. These kernels are invariant under changes in longitude of the central pixel, the latitude being held fixed, as one may have expected.

### 3.6 The non-locality of the real space operators

In the previous section we presented a quantitative understanding of the azimuthal dependence of the real space kernels, providing little insight into their radial dependence. The radial part of these kernels determines the non-locality of the respective operators and encodes all their multipole dependencies. For illustration the radial kernels  $\mathcal{M}f$ ,  $\mathcal{D}f$  &  $\mathcal{I}f$  are

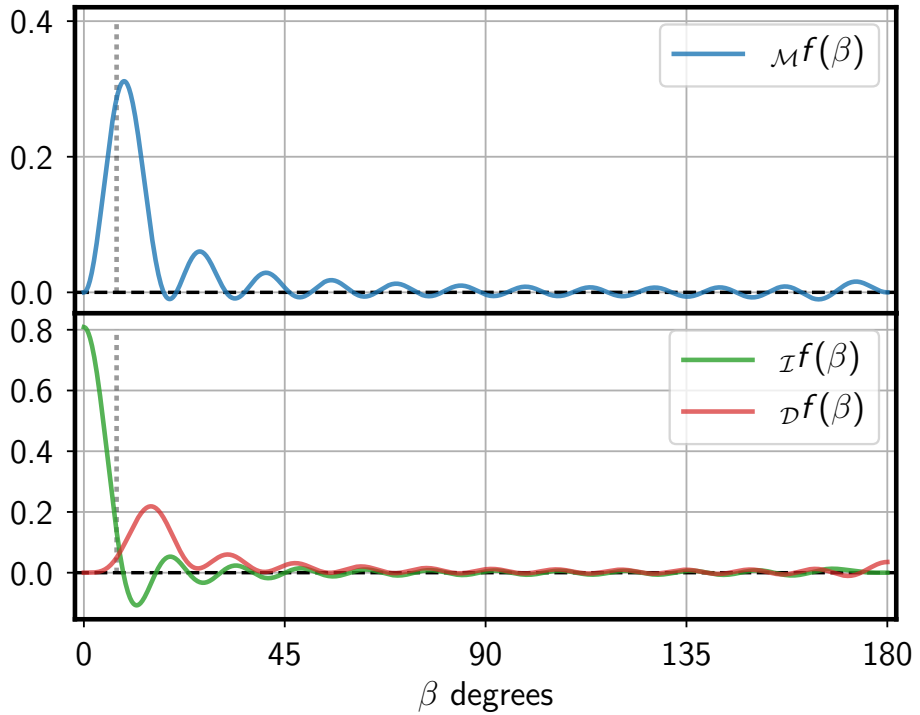


**Figure 4:** The figure depicts the radial part of the convolution kernels. These radial function have been evaluated with the band limit fixed at  $\ell \in [2, 24]$ . The vertical dashed line marks the approximate Healpix pixel size of a NSIDE=8, which is the lowest resolution that allows access to  $\ell_{\max} = 24$ .

evaluated using the respective multipole sums given in Eq. (3.10b) and Eq. (3.27) in the band limit  $\ell \in [2, 192]$  and the resultant functions are depicted in Fig. 4.

$Mf$  is the radial part of the kernel that translates the Stokes parameters  $Q$  &  $U$  to scalars  $E$  &  $B$  and vice versa and it has a vanishing contribution from the regions where  $(\beta \rightarrow 0)$  and from regions  $(\beta \rightarrow \pi)$  as seen in Fig. 4. This can be understood as arising from the fact that the coordinate dependence of the Stokes parameters cannot uniquely integrated out since the Euler angles  $\alpha$  &  $\gamma$  are not uniquely defined at the locations  $\beta = 0, \pi$ . This nature of  $Mf$  is critical to ensure that the derived fields have the necessary spin properties.

$If$  is the radial part of the band limited delta function  $\mathcal{I}$  and expectedly has its maxima at  $\beta = 0$  and decays with increasing angular separation.  $Df$  has a vanishing value in the region where  $\beta \rightarrow 0$  however it does not vanish at  $\beta \rightarrow \pi$  as seen in Fig. 4. The main take away from these observations of the nature of the radial part of the kernel is that the real space operators which decompose the Stokes parameters into parts that correspond to E and B modes are necessarily non-local.

*The band limit dependence:* We further quantify this non-locality by studying the radial extent of the kernels and its dependence on the maximum multipole accessible for analysis. To carry out this study we evaluate the radial functions for different values of  $\ell_{\max}$ , while keeping the lowest multipole fixed at  $\ell_{\min} = 2$ .

The resultant set of radial function are depicted in Fig. 5, where all the function have

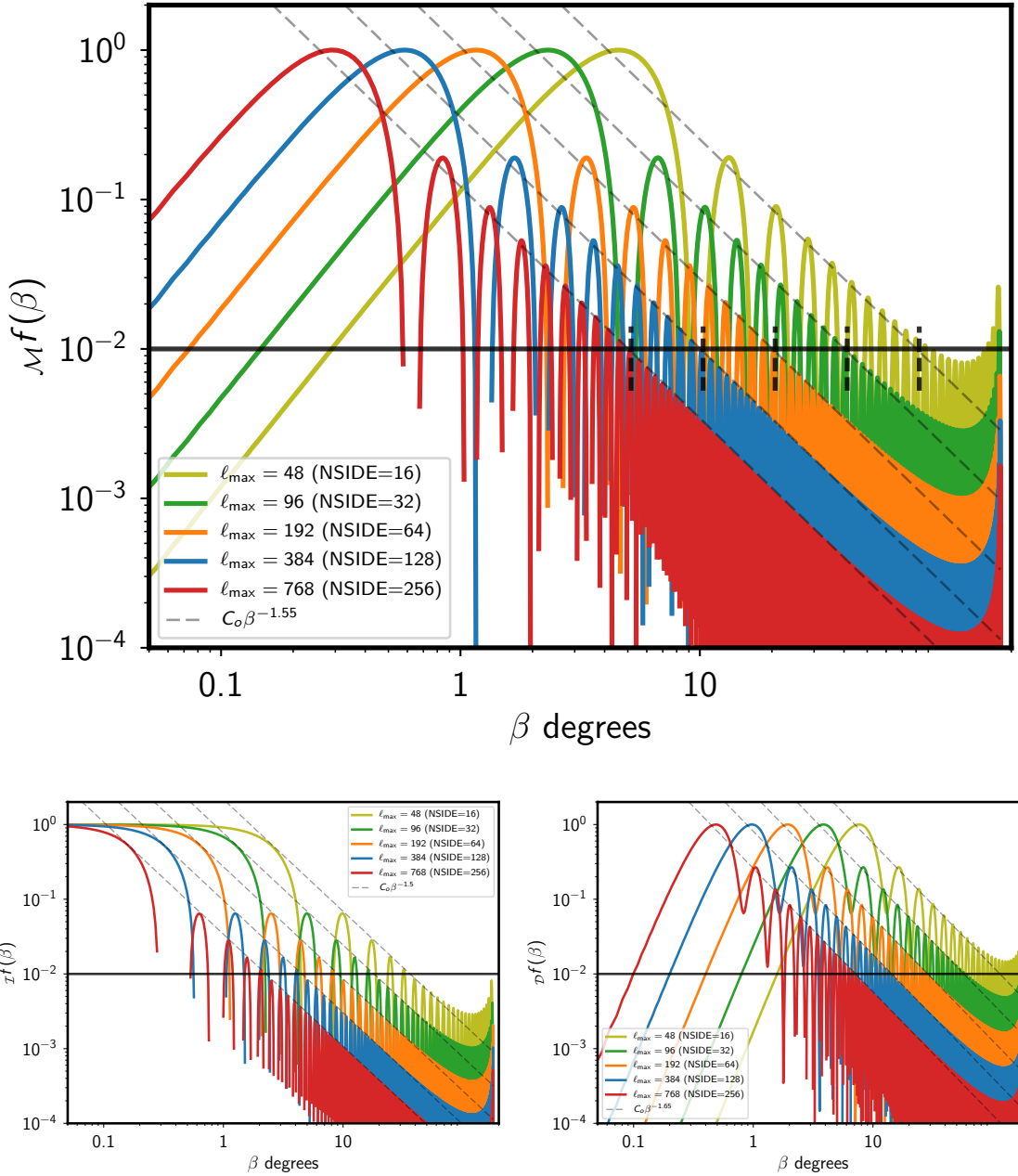


**Figure 5:** The top panel depicts the radial function  $\mathcal{M}f(\beta, \ell_{\min}, \ell_{\max})$  while the bottom left and right panels show the radial functions  $\mathcal{I}f(\beta, \ell_{\min}, \ell_{\max})$  &  $\mathcal{D}f(\beta, \ell_{\min}, \ell_{\max})$  respectively, for fixed  $\ell_{\min} = 2$  and varying  $\ell_{\max}$  as indicated by their legends. All the curves are normalized such that their maxima is set to unity. The horizontal solid black line marks the location where the amplitude of the respective kernels fall below 1% of its maximum. The thin slanted gray lines indicate a power law fit (by eye) to the envelope of the radial functions. The thick black short vertical dashed lines indicate the transition points as predicted by the empirically derived relation for the non-locality parameter  $\beta_0 = \min(180, 180 \frac{22}{\ell_{\max}})$ .

been normalized such that their global maxima is set to unity. The amplitude of these radial function scales up as  $\propto \ell_{\max}^2$ . Note that on increasing  $\ell_{\max}$  the radial kernels shift left, attaining their global maxima at progressively small angular distances  $\beta$ . At intermediate values of  $\beta$ , the envelope of the radial functions is fit well by a power law  $\propto \beta^{-n}$  as seen in Fig. 5. In fact these finding are neatly summarized in the observation that the radial functions computed by evaluating the multipole sums to different maximum multipoles are self similar and follow this interesting telescoping and scaling property,

$${}_rf(\beta, 2, \ell_{\max}) \approx \left[ \frac{\ell_{\max}}{\ell'_{\max}} \right]^2 {}_rf(\beta' = \frac{\ell'_{\max}}{\ell_{\max}} \beta, 2, \ell'_{\max}),$$

where  ${}_rf$  denotes all the different radial functions.

It is useful to define a characteristic radius of the region from which the evaluated resultant fields get most of their contribution. Our primary interest is in quantifying the non-locality of the scalar modes  $E$  &  $B$ , therefore we define the abscissa at which the function  $\mathcal{M}f(\beta, \ell_{\min} = 2, \ell_{\max})$  transits to being monotonously below 1% of the maxima of the function as the non-locality parameter:  $\beta_o$ . The simple empirical derived relation:  $\beta_o = \min(180, 180 \frac{22}{\ell_{\max}})$  provides a reasonable estimate of this transition point for  $\mathcal{M}f$ . This empirical function also provides a reasonable estimate for the transition point for the function  $\mathcal{D}f$  particularly for high  $\ell_{\max}$  and it systematically over-predicts the transition point for the function  $\mathcal{I}f$  as seen in Fig. 5.

**Polarization signature of magnetized filaments** Naturally describes the reason for a positive T/E correlation. Figure 6.

### 3.6.1 Generalized operators

In this section we present a systematic method to generalize the real space operators that translate between  $Q/U$  and  $E/B$  description of CMB polarization. The azimuthal part of the real space kernels is constrained to be of the form  $\sim e^{\pm i2\alpha}$ . The shape of the radial part of the operator is determined by the basis functions and varies as a function of the band limit. It is here that we may potentially choose alternate forms for the radial functions to suit certain kind of analysis.

We can systematically generalize the real space operator by introducing the following harmonic space operator,

$$\tilde{\mathcal{G}} = \begin{bmatrix} g_\ell^E & 0 \\ 0 & g_\ell^B \end{bmatrix}, \quad (3.33)$$

where the functions  $g_\ell^E$  and  $g_\ell^B$  represent the harmonic representation of the modified radial functions and can in the most general case be chosen to be different for  $E$  and  $B$  modes. To simplify discussions and without loosing generality we proceed by setting  $g_\ell^E = g_\ell^B = g_\ell$ . Given this harmonic function  $g_\ell$ , we can define the real space operator  $\bar{O}'$  which translates Stokes  $Q$  &  $U$  to scalars  $E$  &  $B$  and the inverse operator  $\bar{O}'^{-1}$  in the following manner,

$$\bar{O}' = {}_0\mathcal{Y} * \tilde{T}^{-1} * \tilde{\mathcal{G}} * {}_2\mathcal{Y}^\dagger * \bar{T}, \quad (3.34a)$$

$$\bar{O}'^{-1} = \bar{T}^{-1} * {}_2\mathcal{Y} * \tilde{\mathcal{G}}^{-1} * \tilde{T} * {}_0\mathcal{Y}^\dagger \quad (3.34b)$$

where we have used the primed notation to distinguish these generalized operators from the default operators defined in Sec. 3.2 and Sec. 3.3. Requiring both the forward and inverse operators to be well defined constrains the choice of  $\tilde{\mathcal{G}}$  to be such that it has a valid inverse.

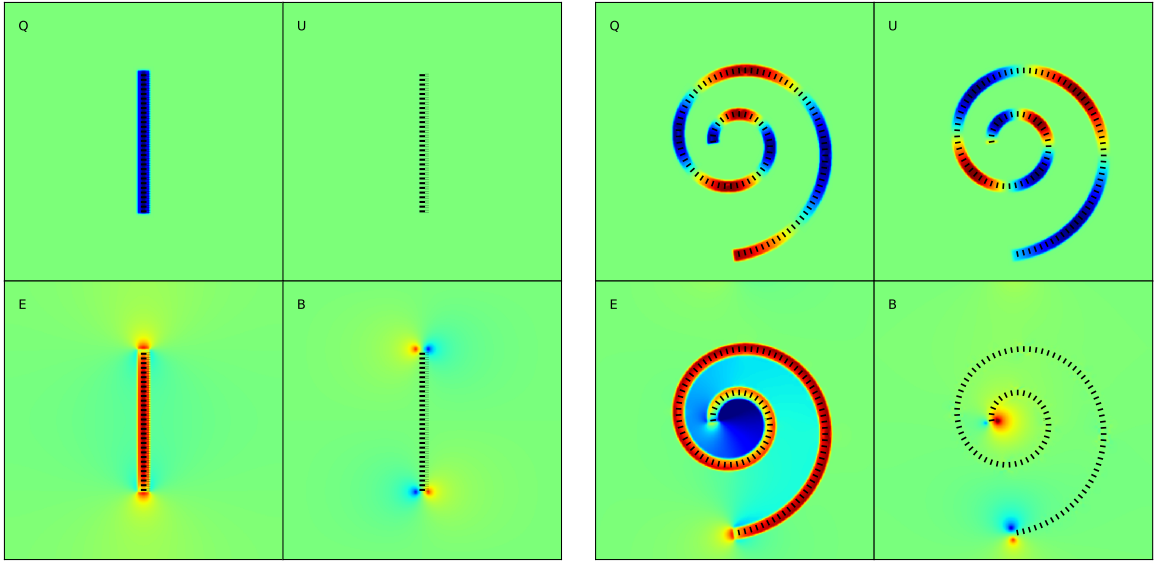


**Figure 6:** The polarization signals of toy filament structures. In a filament organized perfectly along a magnetic field line, the polarization will be perpendicular to the filament direction. The  $E/B$  modes of filaments are in some ways easier to think about than the Stokes parameters. Left panels: in a straight filament, the  $E$ -mode is positive along the filament and at the ends, but negative along the sides.  $B$ -modes are only non-zero at the ends. Right panels: in a curved filament, the  $E$ -mode is again positive along the filament. Outside the filament, the  $E$ -mode is more negative on the interior of the curve than the exterior. The  $B$ -modes are again non-zero only at the ends, and are akin to the straight filament case. In all images, the longitude increases to the left (sky convention).

This is an important criteria to recover the standard CMB spectra. The radial parts of this generalized operator and its inverse are given by the following expressions,

$$G_{QU \rightarrow EB}(\beta) = G(\beta) = \sum_{\ell=2}^{\ell_{\max}} g_\ell \frac{2\ell+1}{4\pi} \sqrt{\frac{(\ell-2)!}{(\ell+2)!}} P_\ell^2(\cos \beta), \quad (3.35a)$$

$$G_{EB \rightarrow QU}(\beta) = G^{-1}(\beta) = \sum_{\ell=2}^{\ell_{\max}} g_\ell^{-1} \frac{2\ell+1}{4\pi} \sqrt{\frac{(\ell-2)!}{(\ell+2)!}} P_\ell^2(\cos \beta). \quad (3.35b)$$

The default radial function is just a special case resulting from the choice  $\tilde{\mathcal{G}} = \mathbb{1}$  ( $g_\ell = 1$ ), in which case  $\tilde{\mathcal{G}}^{-1} = \tilde{\mathcal{G}}$  and therefore  $G^{-1}(\beta) = G(\beta) = \mathcal{M}f$ .

While defining these generalized operators, it is more natural to choose the real space function  $G(\beta)$ , bearing in mind the constraint that  $G(\beta = 0) = G(\beta = \pi) = 0$ . Employing the orthogonality property of associated Legendre polynomials it can be shown that the harmonic function  $g_\ell$  is given by the expression,

$$g_\ell = 2\pi \sqrt{\frac{(\ell-2)!}{(\ell+2)!}} \int_0^\pi G(\beta) P_\ell^2(\cos \beta) d\cos \beta. \quad (3.36)$$

An arbitrary  $G(\beta)$  for which  $g_\ell \neq 1$  can be equivalently thought in terms of the standard  $E$  and  $B$  fields being convolved with some effective circularly symmetric instrument beam

whose radial profile is given by the expression,

$$B(\beta) = \sum_{\ell=0}^{\ell_{\max}} \frac{2\ell+1}{4\pi} g_\ell P_\ell^0(\cos \beta), \quad (3.37)$$

where  $g_\ell$  is the same harmonic function as that appearing in Eq. (3.35). In contrast to the radial function  $G(\beta)$  an instrumental beam function appropriately normalized has the property  $B(\beta) \rightarrow 1$  as  $\beta \rightarrow 0$ . Though the real space behavior of these two function  $G(\beta)$  and  $B(\beta)$  has these differences, in harmonic space they play identical roles.

Therefore it is possible to interpret the beam harmonic coefficients as those representing some modified radial kernel. Fig. 7(ii) depicts the harmonic functions  $g_\ell$  for the respective radial kernel and beams. The modified radial kernel resulting from Gaussian beams with fwhm = 15' & 12' are depicted in Fig. 7(i) as blue and orange curves respectively. Note that instruments beams tend to increase the non-locality parameter  $\beta_0$ , indicated by the shifting right of the maxima of the respective kernels, as one may have expected. The red curve depicts a modified radial kernel which by construction has a very small  $\beta_0$ . Note that the beam function corresponding to the default radial kernel ( $g_\ell = 1$ ) is merely a band limited representation of the delta function beam. Fig. 7(iii) depicts the radial profile of the effective beams corresponding to the different radial kernels.

### 3.6.2 Recovering the default $E$ and $B$ mode spectra

The generalized convolution kernels defined in the previous section, when operated on the Stokes vector returns some scalar  $E'$  and  $B'$  mode maps,

$$\bar{S}' = \bar{O}' * \bar{P} \quad (3.38)$$

which are merely filtered version of the standard  $E$  and  $B$  modes maps. Since the harmonic functions  $g_\ell$  of the modified radial function  $G(\beta)$  can be simply interpreted as the harmonic coefficients of some azimuthally symmetric beam, the spectra of the scalar fields  $E'$  and  $B'$  are related to the spectra of the standard  $E$  and  $B$  fields via the following relation,

$$C_\ell^{EE, BB, EB} = C_\ell^{E'E', B'B', E'B'} / g_\ell^2, \quad (3.39a)$$

$$C_\ell^{TE, TB} = C_\ell^{TE', TB'} / g_\ell, \quad (3.39b)$$

where  $C_\ell$  denotes the angular power spectra and  $T$  refers to the temperature anisotropy map. Therefore the standard CMB spectra can be always recovered as long as the  $1/g_\ell$  &  $1/g_\ell^2$  are well behaved functions, which can be ensured by making a suitable choice for the modified radial function  $G(\beta)$ . Some examples forms of  $G(\beta)$ , its harmonic representation  $g_\ell$  (and its inverse  $1/g_\ell$ ) and the corresponding beam  $B(\beta)$  are depicted in Fig. 7.

### 3.6.3 Relation to the spin raising $\bar{\partial}^2$ and lowering $\bar{\partial}^2$ operators

Recall that's on operating twice with the spin lowering operator on the Stokes charge  $-_2X$  results in filtered version of  $E/B$  maps as in Eq. (2.4). We can construct a modified real space operator by choosing the harmonic space function to be  $g_\ell = \sqrt{\frac{(\ell+2)!}{(\ell-2)!}}$ , resulting in similarly filtered  $E/B$  maps as follows,

$$[\mathcal{E} + i\mathcal{B}](\hat{n}_e) = -\Delta\Omega \sum_{q=1}^{N_{\text{pix}}} \left\{ \left[ \sum_{\ell=\ell_{\min}}^{\ell_{\max}} \frac{2\ell+1}{4\pi} P_\ell^2(\beta_{qe}) \right] e^{-i2\alpha_{eq}} {}_2X(\hat{n}_q) \right\}. \quad (3.40)$$

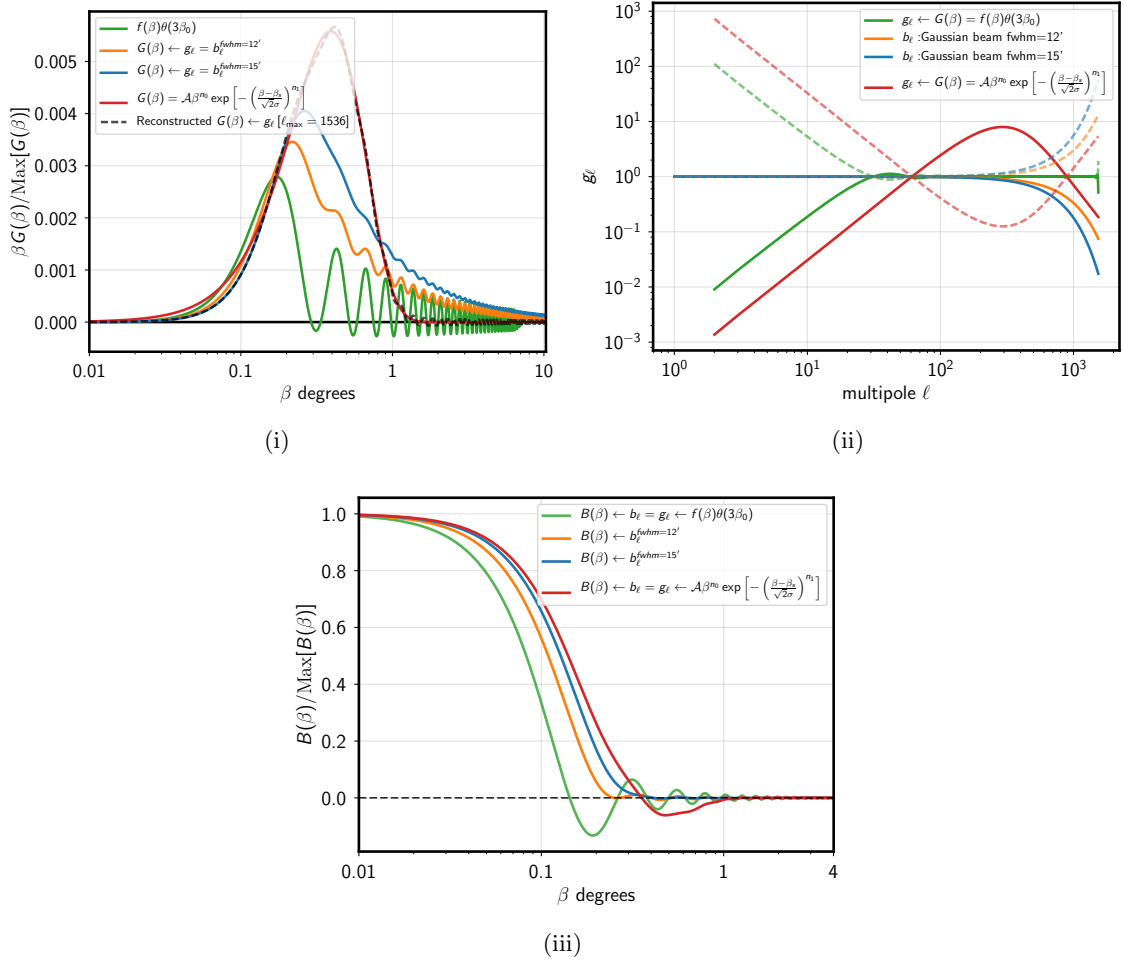


**Figure 7:** Top left: The green line depicts the default radial kernel  $f(\beta)$  defined in Eq. (3.10), multiplied by an apodized step function  $\theta(3\beta_0)$ . The blue and orange lines depict the modified radial function resulting the beam harmonics  $b_\ell$  corresponding to Gaussian beams with fwhm=15 & 12 arc-minutes respectively. The red curve depicts an example modified radial function:  $G(\beta) = A\beta^{n_0} \exp\left[-\left(\frac{\beta-\beta_s}{\sqrt{2}\sigma}\right)^{n_1}\right]$  with parameters set to the following values  $[n_0 = 1; \beta_s = 0; \sigma = 0.004; n_1 = 1.5]$ . The black dashed curve depicts the band limited reconstruction of the modified radial function. Top right: This figure depicts the harmonic representation of the respective radial functions as indicated by the legend. The dashed curves of the corresponding color depict the inverse of the harmonic functions. Bottom: This figure depicts the normalized beam function  $B(\beta)$  evaluated from interpreting the respective harmonic functions as those corresponding to an effective instrument beam.

Comparing Eq. (2.4a) to Eq. (3.40) makes apparent the following mapping,

$$\bar{\partial}^2 \equiv \Delta\Omega \sum_{q=1}^{N_{\text{pix}}} \left[ \sum_{\ell=\ell_{\min}}^{\ell_{\max}} \frac{2\ell+1}{4\pi} P_\ell^2(\beta_{qe}) \right] e^{-i2\alpha_{eq}}. \quad (3.41)$$

The operator  $\bar{\partial}^2$  is composed of derivative operations and hence has an implicit bi-positional dependence for all numerical purposes which is made explicit in the band limited version of the operator. The band limited version of the spin raising operator  $\bar{\partial}^2$  is derived by merely taking the conjugate of the above equation.

## 4 Discussion

A similar equation for real space  $E$  &  $B$  operators was derived in [1], however those results were derived for the flat sky case and did not explicitly derive the radial kernel.  $\Rightarrow$  A discussion on this should be in the conclusions.

In this article we have cast the standard CMB polarization analysis operations in a vector matrix notation. Using this concise notation we derive the real space operators that translate the Stokes vector  $\bar{P}$  to the vector of scalars  $\bar{S}$  and vice versa. We explicitly demonstrated that this real space operation can be simply interpreted as a convolution over the complex field  $[Q - iU]$  (or  $[E + iB]$ ) with an effective complex beam which is fully expressed in terms of the  $Y_{\ell 2}$  spherical harmonic functions. We also use this vector matrix notation to derive real space operators which allow the direct decomposition of the full Stokes vector  $\bar{P}$  into the vector  $\bar{P}_E$  and  $\bar{P}_B$  that correspond to the respective scalar modes.

Given the effective beam interpretation of these real space operators we derive the harmonic coefficients of these effective beams at the north galactic pole. Using these harmonic coefficients we provide a prescription for computing the convolution kernels at any position on the sphere using the standard Healpix built in functions. The procedure is equivalent to parallel transporting the beam at the north pole to any desired location on the sphere. We implement the prescription to compute the kernel at different location on the sphere and provide simple explanations in terms of Euler angles for the observed variations.

These real space convolution kernels provide a spatially intuitive way of understanding the construction of the scalar modes. We explicitly show that the kernels separates into an band limit independent azimuthal operation around any given direction which is primarily responsible for requisite decomposition, while the band limit dependent radial weights can be interpreted as some isotropic smoothing operation. These radial weights primarily determine the non-local dependence of the construction of the respective fields at any location on the Stoke field. We define the parameter  $\beta_0$  as a means to characterize the non-locality and show that  $\beta_0$  scales  $\propto \ell_{\max}^{-1}$ . We show that this non-locality parameter also characterized the non-locality of the  $\bar{O}_{E/B}$  operators.

Finally we present the generalized real space operators  $\bar{O}'$ , which are derived by allowing the radial function to vary from its default form. We derive constraints on the modifications to these radial function by demanding the inverse operator to be well defined. We argue that these modifications to the radial kernel can be interpreted as a some smoothing smoothing operation on the scalar fields with a circularly symmetric instrument beam. We also show that as long as these radial function are invertible, the standard spectra can always be recovered from these modified  $E'$  &  $B'$  maps. The main advantage of modifying these radial function is the ability to generate more locally defined  $E$  and  $B$  mode maps. This could potentially be useful in reducing foreground contamination on large angular scales in a full sky  $E/B$  analysis. Also defining more locally constructed scalar fields  $E$  &  $B$  can be used to circumvent the power leakage nuisance. We explore and demonstrate the working of these ideas in the next paper in this series.

## Acknowledgments

This work was supported by NASA Astrophysics Theory Program under grant NNX17AF87G. We thank David C. Collins for useful discussions.

## A Appendix

### A.1 Product of spin spherical harmonics

The spin spherical harmonics are related to the Wigner D functions via the following relations,

$$D_{-sm}^{\ell}(\alpha, \beta, \gamma) = \sqrt{\frac{4\pi}{2\ell+1}} s Y_{\ell m}(\beta, \alpha) e^{-is\gamma}, \quad (\text{A.1})$$

where  $\alpha, \beta$  &  $\gamma$  can be thought of as Euler angles for some rotation.

The product of two different spherical harmonic functions can be expressed in terms of the Wigner D functions and simplified using their identities. In particular we are interested in products of spherical harmonic function of the following kind,

$$\sum_m s_1 Y_{\ell m}(\theta_e, \phi_e) s_2 Y_{\ell m}^*(\theta_q, \phi_q) = \frac{2\ell+1}{4\pi} \sum_m D_{-s_1 m}^{\ell}(\phi_e, \theta_e, 0) D_{-s_2 m}^{*\ell}(\phi_q, \theta_q, 0), \quad (\text{A.2a})$$

$$= \frac{2\ell+1}{4\pi} \sum_m D_{-s_1 m}^{\ell}(\phi_e, \theta_e, 0) D_{m-s_2}^{\ell}(0, -\theta_q, -\phi_q), \quad (\text{A.2b})$$

$$= \frac{2\ell+1}{4\pi} D_{-s_1-s_2}^{\ell}(\alpha_{qe}, \beta_{qe}, \gamma_{qe}), \quad (\text{A.2c})$$

$$= \sqrt{\frac{2\ell+1}{4\pi}} s_1 Y_{\ell-s_2}(\beta_{qe}, \alpha_{qe}) e^{-is_1\gamma_{qe}} \quad (\text{A.2d})$$

where we have used some standard identities of the Wigner D functions to transition between them equations [4]. Note that the Euler angles  $(\alpha, \beta, \gamma) = (0, -\theta_q, -\phi_q)$  correspond to a rotation that aligns the local cartesian coordinate at  $\hat{n}_q$  with that at the pole and the Euler angles  $(\alpha, \beta, \gamma) = (\phi_e, \theta_e, 0)$  correspond to rotations that align the local cartesian coordinates at the pole with those at the location  $\hat{n}_e$ . Hence the net rotation operation is that of aligning the local cartesian coordinates at location  $\hat{n}_q$  with those at location  $\hat{n}_e$  and therefore the final results are expressed in terms of Euler angles:  $(\alpha_{qe}, \beta_{qe}, \gamma_{qe})$ .

Since the following equation holds true,

$$\sum_m s_1 Y_{\ell m}(\theta_e, \phi_e) s_2 Y_{\ell m}^*(\theta_q, \phi_q) = \sum_m -s_1 Y_{\ell m}^*(\theta_e, \phi_e) -s_2 Y_{\ell m}(\theta_q, \phi_q), \quad (\text{A.3})$$

this sum over product of spin spherical harmonic functions can be equally expressed in terms of the Euler angles corresponding to the inverse rotations. Using the same algebra as given above, it is possible to show that

### A.2 Relation between the real space operators and the spin raising/lowering operators

## References

- [1] M. Zaldarriaga, *The nature of the E-B decomposition of CMB polarization*, *Phys. Rev. D* **64** (jun, 2001) 103001, [[0106174](#)].

- [2] M. Zaldarriaga and U. Seljak, *All-sky analysis of polarization in the microwave background*, *Phys. Rev. D* **55** (feb, 1997) 1830–1840, [[astro-ph/9609170](#)].
- [3] J. N. Goldberg, A. J. Macfarlane, E. T. Newman, F. Rohrlich and E. C. G. Sudarshan, *Spin-s Spherical Harmonics and  $\delta$* , *J. Math. Phys.* **8** (nov, 1967) 2155–2161.
- [4] D. A. Varshalovich, A. N. Moskalev and V. K. Khersonskii, *Quantum Theory of Angular Momentum* (World Scientific). World Scientific, 1988.